Structural and optical properties of Tris(8-hydroxyquinoline) aluminum (III) (Alq 3) thermal evaporated thin films

ARTICLE *in* JOURNAL OF ALLOYS AND COMPOUNDS · SEPTEMBER 2010

Impact Factor: 3 · DOI: 10.1016/j.jallcom.2010.07.110

3 AUTHORS:

Mahmoud mohamed El-Nahass
Ain Shams University
184 PUBLICATIONS **2,129** CITATIONS
SEE PROFILE

A.M. Farid
Ain Shams University
26 PUBLICATIONS **299** CITATIONS
SEE PROFILE

Ahmed Atta Atta
Taif University
25 PUBLICATIONS **215** CITATIONS
SEE PROFILE

Journal of Alloys and Compounds 507 (2010) 112–119

Contents lists available at ScienceDirect

Journal of Alloys and Compounds

journal homepage: www.elsevier.com/locate/jallcom

Structural and optical properties of Tris(8-hydroxyquinoline) aluminum (III) (Alq_3) thermal evaporated thin films

M.M. El-Nahass, A.M. Farid*, A.A. Atta

Physics Department, Faculty of Education, Ain Shams University, Roxy, 11757 Cairo, Egypt

ARTICLE INFO

Article history:
Received 6 July 2009
Accepted 14 July 2010
Available online 22 July 2010

Keywords:
Optical properties
Organic materials
Alq_3
Structural properties

ABSTRACT

X-ray diffraction (XRD), transmission electron microscope (TEM) micrographs and optical properties of Tris(8-hydroxyquinoline) aluminum (III) (Alq_3) have been studied. XRD of powder Alq_3 showed that the material has a polycrystalline nature with triclinic structure. The crystal structure and morphology of the as-deposited and annealed (at 473 K for 2 h.) Alq_3 thin films indicated that the as-deposited film is amorphous in nature, while the annealed film has a polycrystalline nature with amorphous background. The molecular structure of the Alq_3 was confirmed by the analysis of (FTIR) spectra. The optical constants such as the refractive index, n, the absorption index, k and the absorption coefficient, α, of both the amorphous and polycrystalline Alq_3 films were determined using spectrophotometric measurements of transmittance (T) and reflectance (R) in the wavelength range (200–2500 nm). The analysis of the data showed an indirect allowed transition energy gaps E_g^{ind} of 2.66 eV and 2.28 eV for the as-deposited and the annealed Alq_3 thin films, respectively. As well as another probability of direct allowed transition was carried out with energy gaps Eg_1^d of 2.82 eV, and Eg_2^d of 4.14 eV for the as-deposited film and Eg_1^d of 2.59 eV, Eg_2^d of 3.88 eV for the annealed films, respectively. Some optical parameters namely molar extinction coefficient (ε_{molar}), oscillator strength (f) and electric dipole strength (q^2) have been evaluated. According to the single oscillator model (SOM), some related parameters such as oscillation energy (E_0), the dispersion energy (E_d), the optical dielectric constant (ε_∞), the lattice dielectric constant (ε_L) and the ratio of free carrier concentration to its effective mass (N/m^*) were estimated. Graphical representation of both the surface and volume energy loss functions and the real optical conductivity as a function of photon energy supports the existence of the mentioned optical transitions.

1. Introduction

Alq_3 enjoys more and more popularity among scientists due to its interesting optical and electrical features like strong luminescence, high electric conductance, low cost and simple technology of fabrication [1]. Therefore, this material is very important in optoelectronic applications such as, photo-detectors OLEDs, flat and flexible color displays and photovoltaic cells.

It is well-known that octahedral complex of the type MN_3O_3, where M is a trivalent metal and N and O stand for the nitrogen and oxygen atoms, respectively, in the quinoline legends, can occur in two different geometric isomers: meridional and/or facial [2].

Three insoluble crystalline phases of Alq_3 namely α-, β-, and γ-Alq_3 have been synthesized [3]. Possibility to design high-luminance low-voltage driven device based on Alq_3 was demonstrated at 1987 [4]. Since that time an intense effort has been dedicated to develop and improve organic electroluminescence diodes (OLEDs) [5]. Alq_3 is a stable material that can be sublimed to grow thin films on large area plastic substrates and stands as one of the most successful materials used in organic electroluminescence applications. Most of the recent studies have been devoted to optimize the device characteristics [6], to improve the morphological stability [7,8], for the understanding of the charge-transport mechanisms [9,10] as well as for tuning of the organic light emitted diode (OLED) emission spectrum [11,12]. Few studies have been devoted to the optical properties of Alq_3, focusing mainly on the solution and sublimed thin film photoluminescence. The aim of the present work is to study the structural and optical properties of thermal evaporated Alq_3 thin films and to deduce the optical parameters using spectrophotometric method of the as-deposited and annealed films. Also, the type of transition is to be identified.

2. Experimental procedure

2.1. Preparation of thin films

The Alq_3 powder used in this study is obtained from (Aldrich). Thin films of Alq_3 of average thicknesses (239 nm) were deposited by thermal evaporation technique, using a high vacuum coating unit (Edwards, E306A). The powder Alq_3 was sublimed

* Corresponding author. Tel.: +20 202 22876569.
E-mail address: ashganfarid@hotmail.com (A.M. Farid).

0925-8388/$ – see front matter © 2010 Elsevier B.V. All rights reserved.
doi:10.1016/j.jallcom.2010.07.110

Table 1
Absorption frequencies in 400–2000 cm^{-1} infrared region for powder, as-deposited and annealed thin film of Alq_3.

Powder $(cm)^{-1}$	As-deposited films $(cm)^{-1}$	Annealed films $(cm)^{-1}$	Assignment
1603.52	1603.52	1603.52	Aromatic C=C bending
1578.45	1578.45	1578.45	Aromatic C=C bending
1498.42	1499.38	1498.42	Aromatic C=C bending
1467.56	1466.6	1467.56	Aromatic stretching C=C
1425.14	1426.1		Aromatic stretching C=C
1381.75	1382.71	1382.71	Aromatic amine
1329.68	1327.75	1328.71	Aromatic amine
1280.5	1279.54	1280.5	Aromatic amine
1230.36	1229.4	1231.33	C–O strong stretching
1176.36	1175.4	1173.47	C–O strong stretching
1113.69	1113.69	1113.69	C–O strong stretching
1055.84	1054.87		C–O strong stretching
1031.73	1031.73	1031.73	C–O strong stretching
957.484			Isoindol deformation
917.95	917.95		Isoindol deformation
862.025	868.774	865.882	C–H bending
826.348	826.348	826.348	C–H bending
	803.206		C–H bending
788.743	789.707	789.707	C–H bending
748.245	748.245	748.245	C–H bending
647.965	647.001	647.965	C–H bending
576.612	576.612	575.647	C–H bending
545.756	545.756	545.756	Stretching Al–O vibration
504.294	503.33		Stretching Al–O vibration
455.118	458.011	460.904	Stretching Al–O vibration
419.442	418.477	418.477	Stretching Al–N vibration

from a quartz crucible source heated by a tungsten coil in a vacuum of 10^{-4} Pa. The film was deposited onto pre-cleaned glass substrate (for structure investigation) and diffused optically flat quartz substrates (for optical investigation). The thickness of the films was determined using a quartz crystal thickness monitor (Edwards, Model FTM4) and calibrated by Tolansky's technique [13]. The as-deposited Alq_3 thin film was annealed at 473 K for 2 h under vacuum of 10^{-1} Pa. A Philips X-ray diffractometer (model X' pert) was used for the measurements of structural properties with utilized monochromatic Cu K_α radiation ($\lambda = 1.5418$ Å) operated at 40 kV and 25 mA. Fourier Transformation Infrared transmission (FTIR) spectra for the powder, the as-deposited and annealed thin films of Alq_3 were studied to confirm the molecular structure of Alq_3 compound. The measurements were performed using (Buker, Vector 22) infrared spectrophotometer in the range 400–2000 cm^{-1}. The morphology of the as-deposited and annealed Alq_3 thin films were studied using transmission electron microscope (TEM) of type (JEOL JEM-1230).

Optical properties were investigated for the as deposited and annealed thin films by spectrophotometric measurements of transmittance, T, and reflectance, R, at normal incidence in the spectral range from 200 to 2500 nm, using a double-beam spectrophotometer (JASCO model V-570 UV–vis–NIR) attached to a specular reflection stage.

2.2. Optical properties

The absolute values of the measured transmittance, T, and reflectance, R, after correction of the absorbance and reflectance of the substrate are given by [14,15]

$$T = \left(\frac{I_{ft}}{I_q}\right)(1 - R_q) \tag{1}$$

where R_q is the reflectance of quartz. I_{ft} and I_q are the intensities of light passing through – quartz system and reference quartz substrate, respectively, and

$$R = \left\{\left(\frac{I_{fr}}{I_m}\right) R_m(1 + [1 - R_q]^2)\right\} - T^2 R_q \tag{2}$$

where I_{fr} and I_m are the intensities of light reflected from the sample and that from reference mirror, respectively, R_m is the reflectance of Al-mirror and R_q is the reflectance of quartz.

The refractive index (n) and the extinction coefficient (k) of the thin films at different wavelengths can be calculated by using the following equations:

$$\alpha = \left(\frac{1}{d}\right) \ln\left[\frac{(1-R)^2}{2T} + \sqrt{\frac{(1-R)^4}{4T^2} + R^2}\right] \tag{3}$$

$$n = \frac{1+R}{1-R} + \sqrt{\frac{4R}{(1-R)^2} - k^2} \tag{4}$$

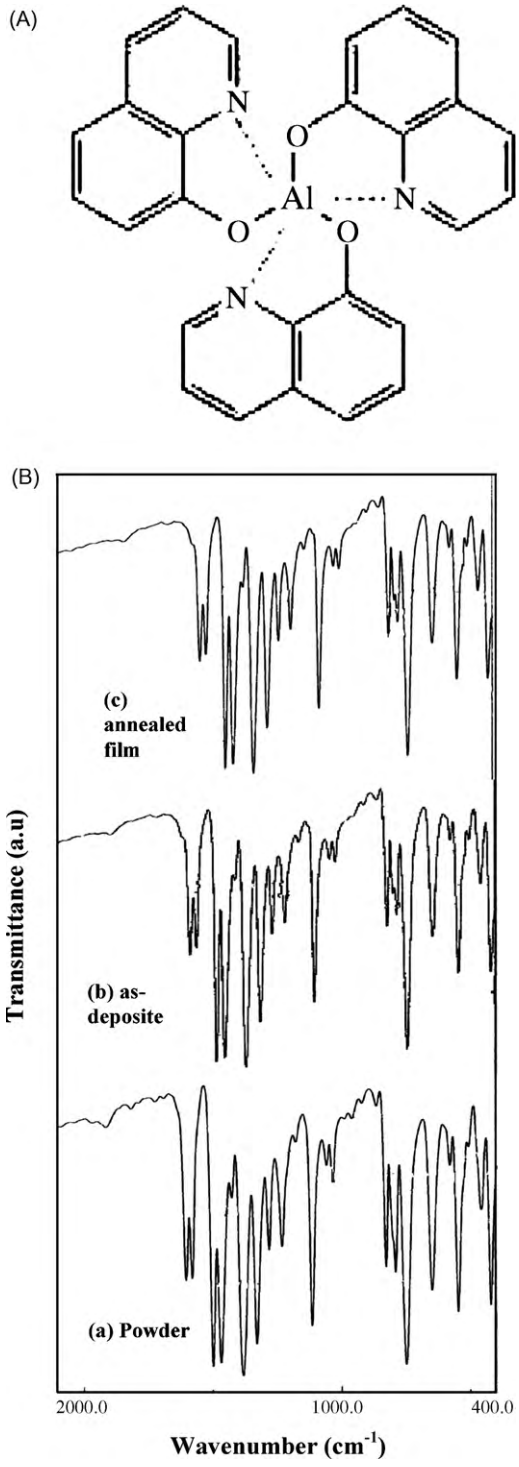

Fig. 1. (A) The chemical configuration of $Alq_3(C_{27}H_{18}AlN_3O_3)$. (B) The infrared spectra of Alq_3 in powder form, as-deposited and annealed (at 473 K for 2 h) thin films.

$$k = \left(\frac{\alpha\lambda}{4\pi}\right)$$

where α is the absorption coefficient and d is the film thickness.

By knowing (d), unique values of (n) and (k) can be obtained. The experimental errors were taken into account as ±5% for the film thickness measurements and ±1% for T and R. The error in the calculated values of n and k were estimated to be ±3% and 2.5%, respectively.

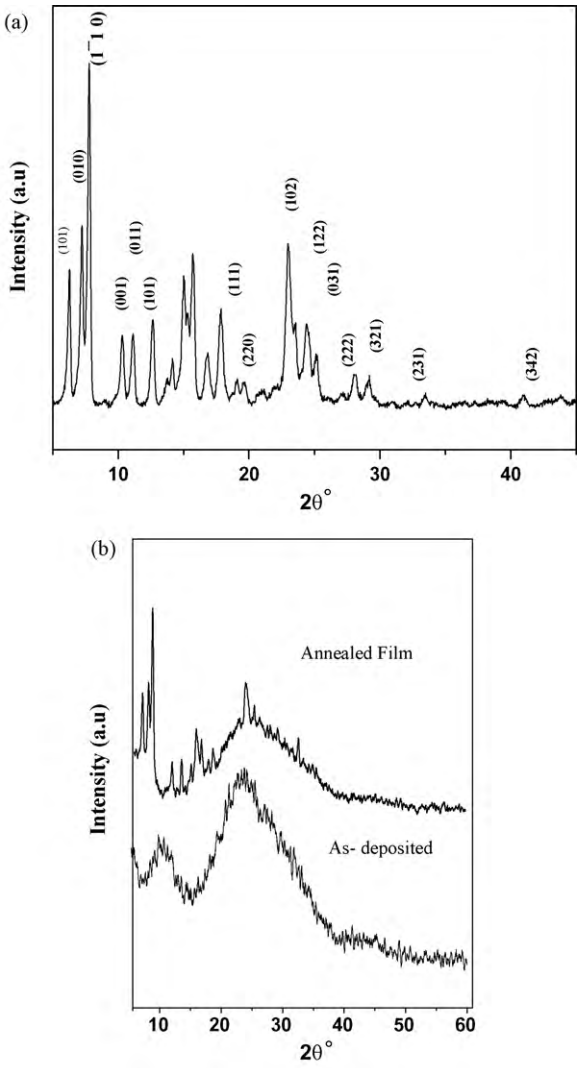

Fig. 2. (XRD) pattern of Alq_3 in the (a) powder form and (b) as-deposited and annealed thin films.

3. Results and discussion

3.1. Structural investigations

3.1.1. (FTIR) spectral study

Fig. 1(A) represents the chemical configuration of Alq3. Fig. 1(B) shows the (FTIR) spectra of the powder, the as deposited (on KBr substrate) and annealed Alq_3 thin films. It is noticed that there is no significant change in the chemical bonding structure for the powder and thermally evaporated thin films (before and after annealing) is observed within the detection limit of (FTIR). This result discloses the thermal stability of Alq_3 and also indicates that the thermal evaporation technique is a good method for the preparation of Alq_3 thin films. These results are also in good agreement with that of Kim et al. [16]. The possible vibrational modes are presented in Table 1. There are no transformation of the aromatic stretching C=C (1600–1450 cm^{-1}) and the aromatic amine resonance C–N–C (1370–1250 cm^{-1}) and this consists with previous results [16–18].

3.1.2. (XRD) analysis

Fig. 2(a) shows the XRD patterns for the powder form of Alq_3. It indicates that the powder form is polycrystalline with the three characteristic planes of the α form, (1 0 1), (0 1 0) and (1 $\bar{1}$ 0), respectively and this is in good agreement with Cölle and Brütting [18]. The indexing of the (XRD) pattern was done using the CRYSFIRE computer program [19]. The analysis of the (XRD) of the powder indicates also that Alq_3 has triclinic structure with space group $P\bar{1}$. The lattice constants are as follows: $a = 10.25$ Å, $b = 13.17$ Å, $c = 8.44$ Å, $\alpha = 97.1°$, $\beta = 89.7°$ and $\gamma = 108.6°$. This also agrees with [18]. Fig. 2(b) shows the (XRD) pattern for the as-deposited and annealed Alq_3 thin films. The figure indicates that the as-deposited film has amorphous nature with a small peak at ($2\theta = 10°$) and a broad peak around ($2\theta = 24°$) and this result agrees with Xu and Xu [17] and Brinkmann et al. [20]. It is noticed also from the figure that the annealed film has a polycrystalline nature with the three characteristic peaks of the α form, (1 0 1), (0 1 0) and (1 $\bar{1}$ 0), respectively.

This indicates that the annealing process change the degree of crystallinity of the as-deposited Alq_3 film.

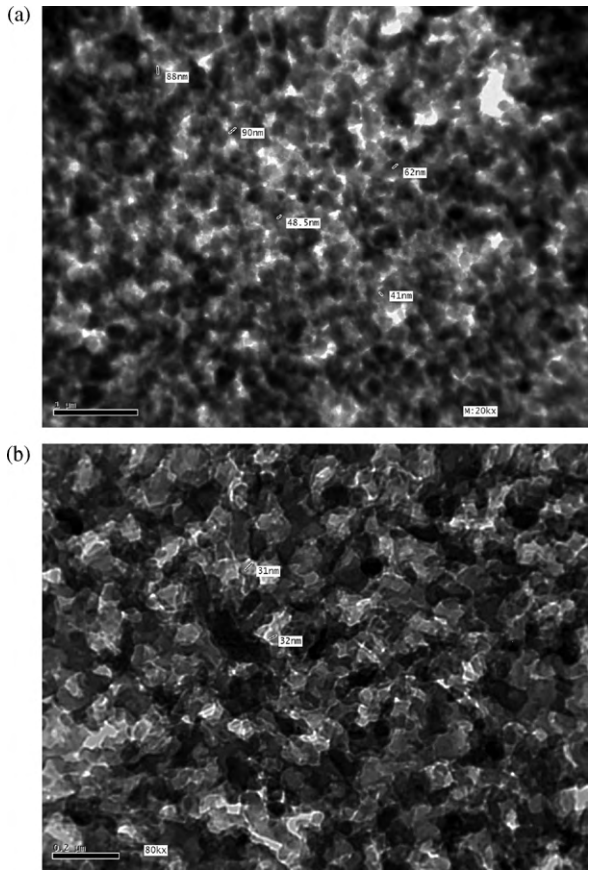

Fig. 3. (TEM) micrographs for (a) as-deposited Alq_3 thin film and (b) annealed Alq_3 thin film.

3.1.3. (TEM) investigations

Fig. 3(a) is the transmission electron micrograph for as-deposited Alq_3 thin film of thickness about (70 nm) at room temperature, which shows small nanoparticles with an average size 60 nm. Fig. 3(b) is the transmission electron micrograph for Alq_3 thin film annealed at 473 K. It indicates that the annealing process caused the nanoparticles of the as-deposited Alq_3 film, to grow and reach an average size about 100 nm (Fig. 3b). Fig. 4(a and b) shows the electron diffraction pattern of the as-deposited and annealed Alq_3 thin films. From the two figures it is noticed that the as-deposited thin film pattern consists of halos that confirm the amorphous nature of Alq_3 thin film. Fig. 4(b) shows the electron diffraction pattern of the Alq_3 film annealed at 473 K for 2 h. The pattern consists of dotty rings which indicate that the film

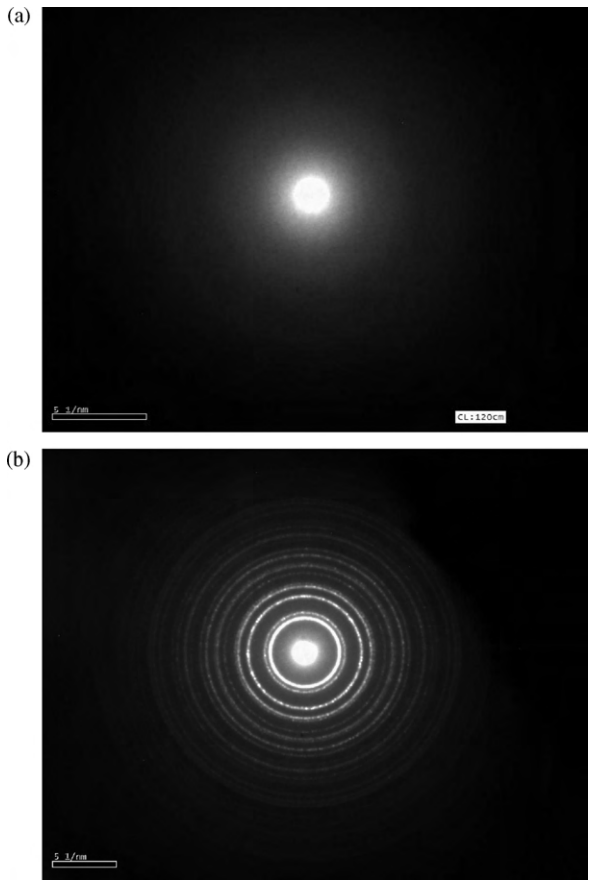

Fig. 4. The diffraction electron microscope patterns for (a) as-deposited Alq_3 thin film (d = 70 nm) and (b) annealed Alq_3 thin film.

is polycrystalline. This also indicates that the annealing process change the degree of crystallinity of the as-deposited Alq_3 film. These results agree also with the (XRD) patterns.

3.2. Optical properties

The spectral behavior of both transmittance (T) and reflectance (R) (for the as-deposited and annealed thin films) of Alq_3, are shown in Fig. 5. The wavelength range was (200–2500) nm and the average film thickness was 239 nm. It is observed that at larger wavelength ($\lambda > 900$ nm) the films become transparent and no light is scattered or absorbed, i.e. ($T + R = 1$). At shorter wavelength ($\lambda < 900$ nm)

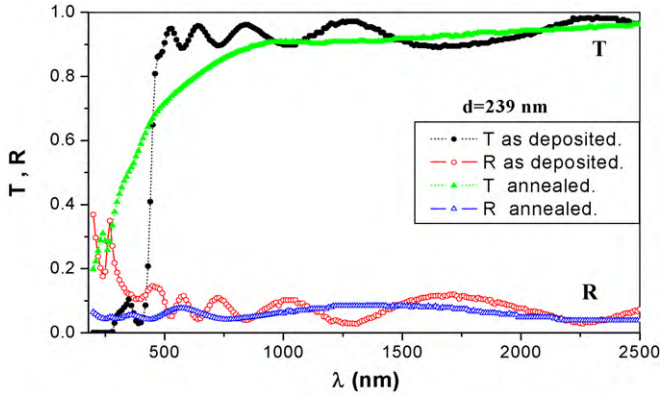

Fig. 5. The spectral distribution of the transmittance $T(\lambda)$ and reflectance $R(\lambda)$for as deposited and annealed of average thickness (239 nm) Alq_3 thin films.

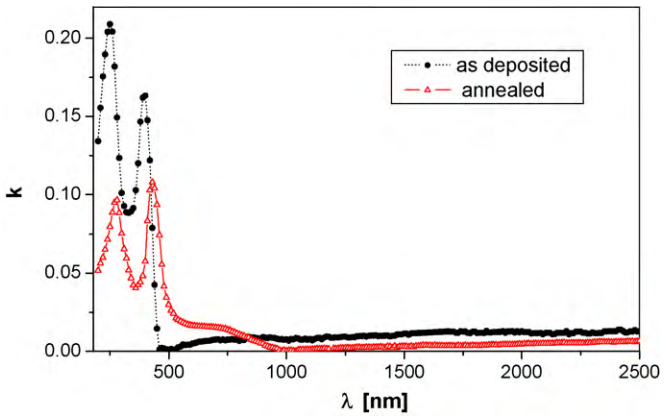

Fig. 6. Spectral distribution of the extinction coefficient (k) for as-deposited and annealed Alq_3 thin films.

absorption takes place, i.e. ($T + R < 1$). Fig. 6 represents the spectral distribution of the absorption index, $k(\lambda)$ for the as-deposited and annealed films of Alq_3. Fig. 7 shows the absorption coefficient, α, which can be calculated from the $k(\lambda)$ data using the formula ($\alpha = 4\pi k/\lambda$). It is useful to relate the absorption coefficient (α) to the molar extinction (ε_{molar}), corresponding to the transition at frequency (ν), which is used to describe the absorption of light by non-solid molecular media [21,22]. If the solid has a concentration of N molecules per unit volume, the absorption coefficient (α) and the molar extinction coefficient (ε_{molar}), will be related by the expression [21]

$$\alpha = \frac{N}{N_{Avo}} \times 10^3 \ln(10)\varepsilon_{molar} = \frac{\rho}{M} \times 10^3 \ln(10)\varepsilon_{molar} = const.\varepsilon_{molar} \quad (5)$$

where N is the number of molecules per unit volume, N_{Avo} is the Avogadro's number, M is the molecular weight of Alq_3, ρ its density and ε_{molar} is in units of liters per mol cm. Some important spectral parameters such as, the oscillator strength (f), the electric dipole strength (q^2) and the absorption half-band width ($\Delta\lambda/\lambda$) for the as deposited and annealed Alq_3 thin films can be calculated using the expressions [23]

$$f = 4.32 \times 10^{-9} \int \varepsilon_{molar}(\nu)d\nu \quad (6)$$

$$q^2 = \left(\frac{1}{2500}\right) \varepsilon_{molar} \left(\frac{\Delta\lambda}{\lambda}\right) \quad (7)$$

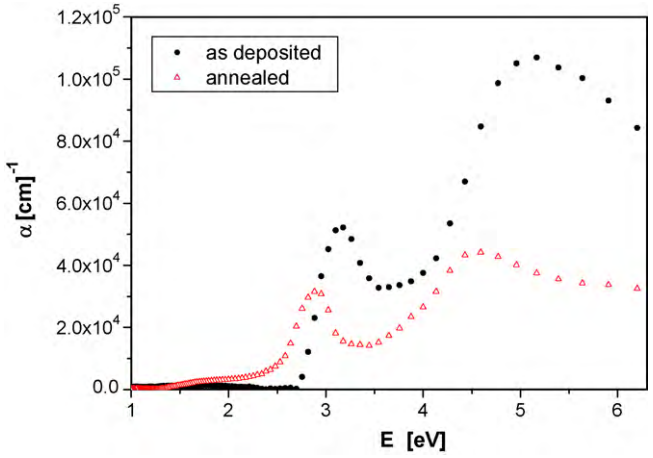

Fig. 7. The variation of the absorption coefficient (α) as a function of the photon energy (E) for the as-deposited and annealed Alq_3 thin films.

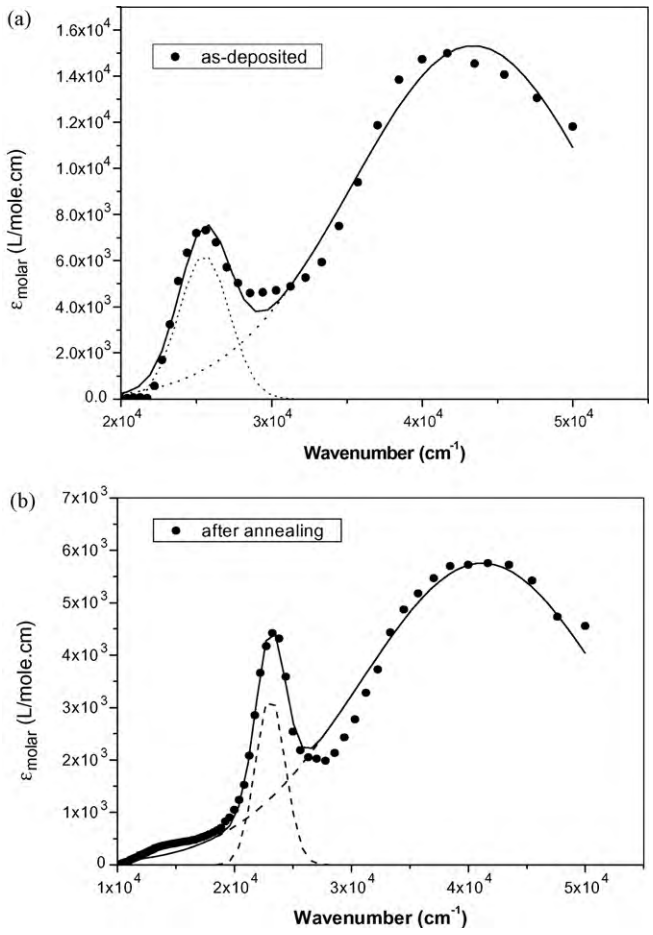

Fig. 8. Molar extinction coefficient (ε_{molar}) for (a) the as-deposited Alq_3 thin film and (b) the annealed Alq_3 thin film.

Table 2
The spectral parameters for different regions for as-deposited and annealed Alq_3 thin films.

Alq_3	E_{peak} (eV)	f	q^2 (Å)^2
As deposited film	3.18	0.12	0.33
	5.39	1.35	2.27
Annealed film	2.88	0.05	0.14
	5.17	0.66	1.17

The calculated parameters are collected in Table 2. From the table it is noticed that the values of (f) and (q^2) decreased by the annealing process.

Fig. 8(a and b) represents the molar extinction coefficient for the as-deposited and annealed Alq_3 films.

The absorption coefficient α for direct band gap material is given by the following relation:

$$\alpha h\nu = A(h\nu - E_g)^r \quad (8)$$

where $h\nu$ is photon energy, A is a constant and E_g is the optical energy gap. The value of r is 1/2 for allowed direct transition

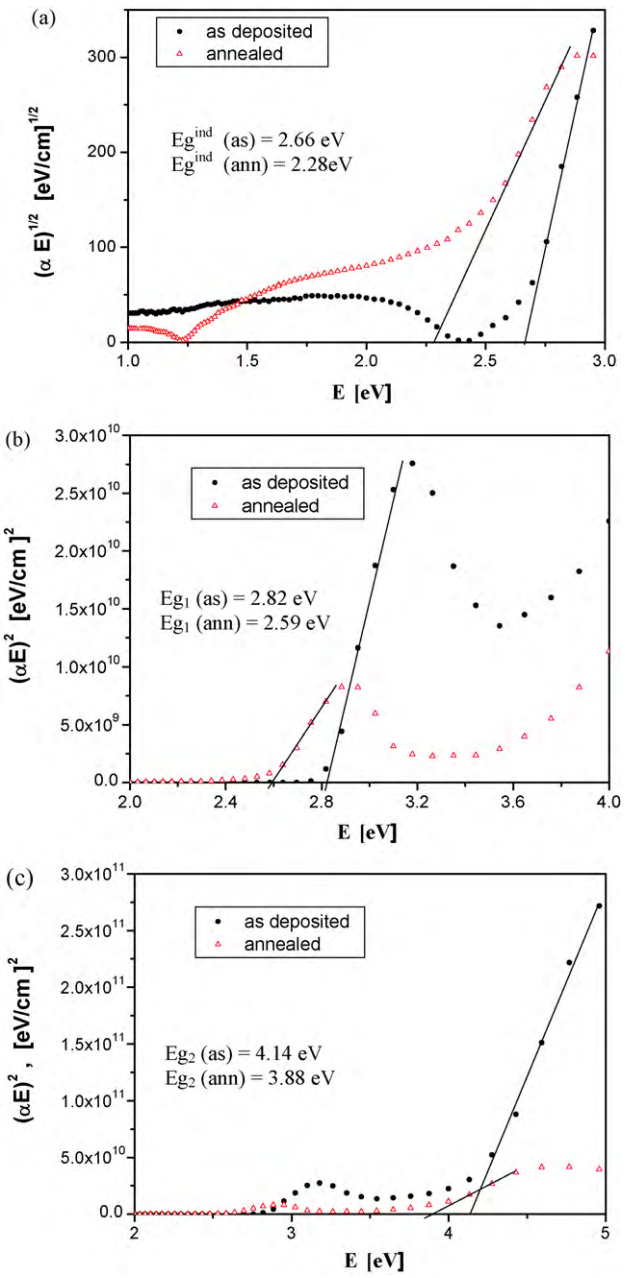

Fig. 9. (a) Plot of $(\alpha h\nu)^{1/2}$ against (E) for the as-deposited and annealed Alq_3 thin films. (b and c) Plot of $(\alpha h\nu)^2$ against (E) for the as-deposited and annealed Alq_3 thin films.

and 3/2 for forbidden transition [24], and $r = 2$ and 3 for indirect allowed and forbidden transition, respectively. The absorption ($\alpha < 10^4$ cm^{-1}) is related to indirect inter-band transitions. The indirect band gap can be determined by plotting $(\alpha h\nu)^{1/2}$ as a function of photon energy ($h\nu$) as shown in Fig. 9(a). The extrapolation of the straight line to $(\alpha h\nu)^{1/2} = 0$ gives the values of the optical band gaps; $E_g^{ind} = 2.66$ eV and 2.28 eV for the as-deposited and annealed

Table 3
The values of (ε_∞), E_0, E_d, (ε_L), N/m^* and the optical energy gaps of as-deposited and annealed thin films of Alq_3.

Alq_3	E_d (eV)	E_0 (eV)	ε_L	ε_∞	(N/m^*) (g^{-1} cm^{-3})	E_{g1}^{ind} (eV)	E_{g1}^{d} (eV)	E_{g2}^{d} (eV)
As-deposited film (present work)	8.257	3.696	3.461	3.234	6.015×10^{46}	2.66	2.82	4.14
Annealed film (present work)	9.417	5.568	2.774	2.69	2.95×10^{46}	2.28	2.59	3.88
As deposited (other Refs.)							3.2 [25]2.8 [1]	4.6 [25]

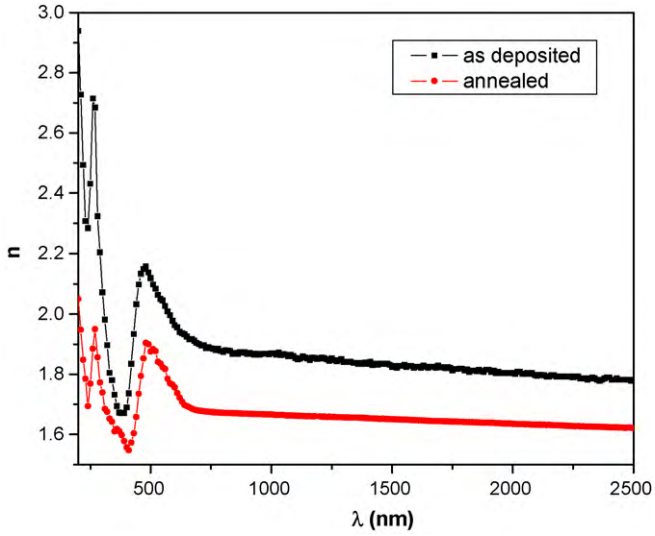

Fig. 10. Spectral distribution of the refractive index (n) for the as-deposited and annealed Alq_3 thin films.

Alq_3 thin films, respectively as seen in Table 3. Also a probability of a direct transition was found by plotting $(\alpha h\nu)^2$ as a function of photon energy ($h\nu$) as shown in Fig. 9(b). The values of the optical energy gaps were calculated as $E_{g1}^{d} = 2.82$ eV and 2.59 eV for the as-deposited and annealed Alq_3 thin films, respectively.

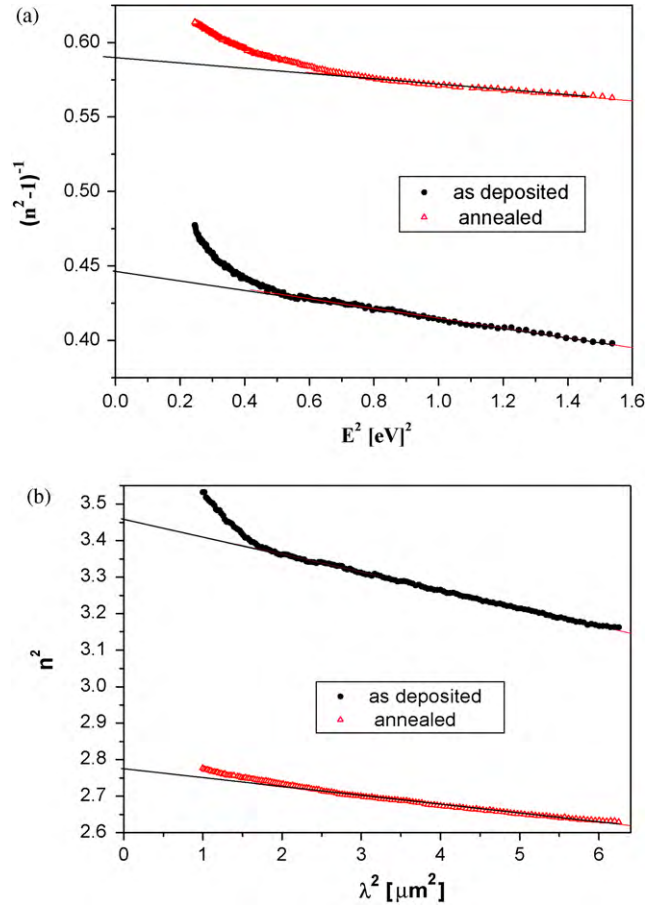

Fig. 11. (a) The variation of $(n^2-1)^{-1}$ against photon energy $(E)^2$ for the as-deposited and annealed Alq_3 thin films. (b) The variation of (n^2) against (λ^2) for the as-deposited and annealed Alq_3 thin films.

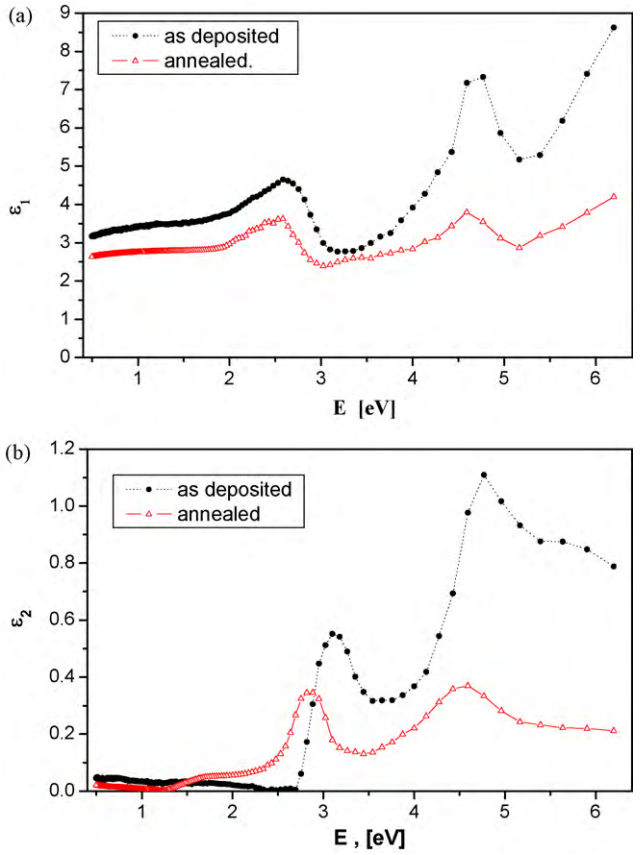

Fig. 12. (a) The real dielectric constant (ε_1) as a function of photon energy (E) for the as-deposited and annealed Alq_3 thin films. (b) The imaginary dielectric constant (ε_2) as a function of photon energy (E) for the as-deposited and annealed Alq_3 thin films.

Another optical energy gaps were obtained from Fig. 9(c) as; $E_{g2}^{d} = 4.14$ eV and 3.88 eV for the as-deposited and annealed Alq_3 thin films, respectively and these results agree with others [25].

The dispersion spectrum for the as deposited and annealed Alq_3 thin film in the wavelength range (200–2500) nm is shown in Fig. 10. It is noticed that there is anomalous dispersion at ($\lambda < 900$ nm), as well as normal dispersion in the wavelength ($\lambda > 900$ nm). The values of the refractive index (n) at ($\lambda = 500$–900 nm) are agree with Dalasiński [1]. In the region of normal dispersion, the single oscillation model (SOM) is applied using relation [26]:

$$n^2(E) - 1 = \frac{E_0 E_d}{E_0^2 - E^2} \tag{9}$$

where E_d is the dispersion energy, E_0 is the single-oscillator energy and E is the photon energy. The parameter E_d is a measure of the intensity of the inter-band optical transition. This parameter does not significantly depend on the band gap. A plot of $(n^2-1)^{-1}$ versus E^2 of the as-deposited and annealed Alq_3 thin film is illustrated in Fig. 11(a). The values of E_d and E_0 are obtained from the slope and the intercept resulting from the extrapolation of the line, the values are given in Table 3.

The optical dielectric constant ($\varepsilon_\infty = n^2$) was calculated (see Table 3).

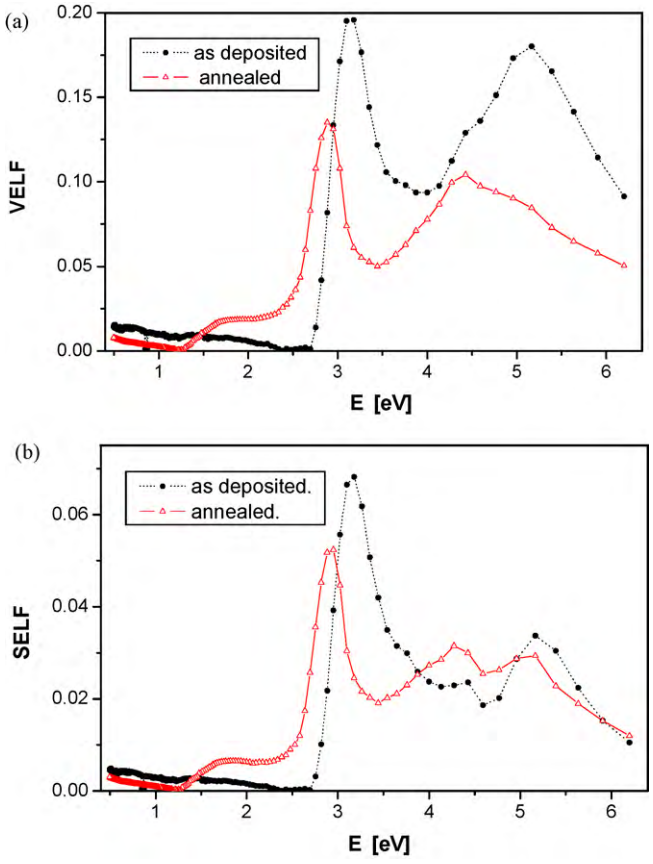

Fig. 13. (a) VELF and (b) SELF for the as-deposited and annealed Alq_3 thin films.

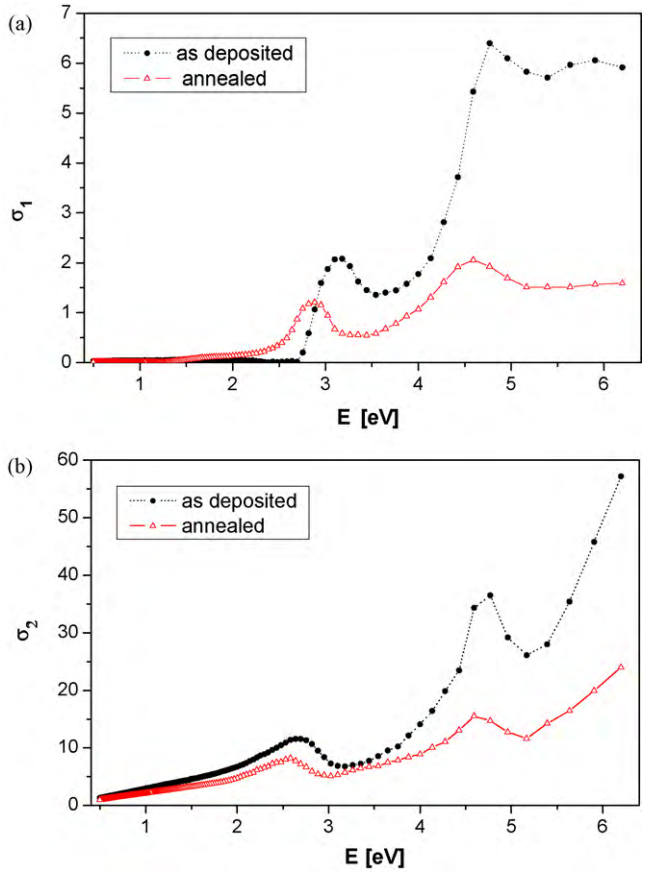

Fig. 14. (a) The real part and (b) the imaginary part of optical conductivity σ_1 for as-deposited and annealed Alq_3 thin films.

The relation between the lattice dielectric constant, ε_L, wavelength, λ, and the refractive index, n, is given by [22]:

$$n^2 = \varepsilon_L - \left(\frac{e^2}{\pi c^2}\right)\left(\frac{N}{m^*}\right)\lambda^2 \quad (10)$$

where ε_L, is the lattice dielectric constant, e is the elementary charge and N/m^* is the ratio of carrier concentration to the effective mass.

By plotting n^2 versus λ^2 as in Fig. 11(b), the values of ε_L and (N/m^*) were determined from the intercept ($\lambda^2 = 0$) and the slope of the line for the as-deposited and annealed films, respectively, as in Table 3. Fig. 12(a and b) represents the real dielectric constant $\varepsilon_1 = n^2 - k^2$ as a function of the energy for the as-deposited and annealed Alq_3 thin films. Also the imaginary dielectric constant $\varepsilon_2 = 2nk$ for as deposited and annealed Alq_3 films is shown in the figure.

It is possible to calculate the volume and surface energy loss function (VELF and SELF) from the relations [27]:

$$\text{VELF} = \frac{\varepsilon_2^2}{\varepsilon_1^2 - \varepsilon_2^2}$$

$$\text{SELF} = \frac{\varepsilon_2^2}{(\varepsilon_1^2 + 1)^2 + \varepsilon_2^2}$$

from Fig. 13(a and b) it is noticed that the VELF values are higher than the SELF of the Alq_3 films. Also the real part of the optical conductivity $\sigma_1 = \varepsilon_2/4\pi$ and the imaginary part $\sigma_2 = (\omega(1 - \varepsilon_1))/4\pi$ are shown in Fig. 14(a and b). The above two Figs. 13 and 14 showed the existence of the possible optical transitions. By using these functions we can confirm that the optical transition occurs by direct transition.

4. Conclusion

The infrared spectra for the powder and thin films of Alq_3 before and after annealing (at 473 K for 2 h) show the stability of the material and also indicate that the thermal evaporation technique is a best method for preparing Alq_3 thin films.

The (XRD) studies of Alq_3 in a powder form indicate that the material is a polycrystalline with triclinic structure and space group $P-1$, for the as-deposited Alq_3 thin films gives a small peak at ($2\theta = 10^\circ$) in amorphous background. While for the annealed Alq_3 thin film it showed that the annealing process increased the crystallinity of the as-deposited film. (TEM) micrographs showed that the annealing process increased the grain size and the crystallinity of the film.

The optical properties of thermally evaporated Alq_3 thin films (as-deposited and annealed at 473 K for 2 h) have been studied. Using the measurements of transmittance and reflectance in the spectral range 200–2500 nm, revealed that electronic transitions were observed, one is either indirect allowed transition with energy gaps 2.66 eV and 2.28 eV for the as-deposited and annealed Alq_3 thin films, respectively, or direct allowed transitions with energy gaps $E_{g1}^d = 2.82$ eV and 4.14 eV for the as-deposited and annealed thin film, respectively and $E_{g2}^d = 2.59$ eV and 3.88 eV for the as-deposited and annealed film, respectively. By using (VELF), (SELF) σ_1 and σ_2 functions we can confirm that the optical transition occurs by direct transition.

Acknowledgment

The authors are grateful to Prof. Dr. F. Abd-El-Salam, Physics Department, Faculty of Education, Ain Shams University, for his valuable cooperation.

References

[1] P. Dalasiński, Z. Łukasiak, M. Wojdyła, M. Rębarz, W. Bała, Opt. Mater. 28 (2006) 98.
[2] G. Kauffmann, Coord. Chem. Rev. 12 (1974) 105.
[3] M. Muccini, M. Brinkmann, G. Godret, C. Taliani, N. Masciocchi, A. Sironi, Synth. Met. 122 (2001) 31.
[4] C.W. Tang, S.A. van Slyke, Appl. Phys. Lett. 51 (1987) 913.
[5] R.H. Friend, R.W. Gymer, A.B. Holmes, J.H. Burroughes, R.N. Marks, C. Taliani, D.A. Dos Santos, J.L. Brėdas, M. Lögdlund, W.R. Salaneck, Nature (London) 397 (1999) 121.
[6] J. McElvain, H. Antoniadis, M.R. Hueschen, J.N. Miller, D.M. Roitman, J.R. Sheat, R.L. Moon, J. Appl. Phys. 80 (1996) 6002.
[7] L.M. Do, E.M. Han, N. Yamamoto, M. Fujihira, Thin Solid Films 273 (1996) 202.
[8] L.M. Do, E.M. Han, N. Yamamoto, M. Fujihira, T. Kanno, S. Yoshida, A. Maeda, A.J. Ikushima, J. Appl. Phys. 76 (1994) 5118.
[9] P.E. Burrows, Z. Shen, V. Bulovic, D.M. McCarty, S.R. Forrest, J.A. Cronin, M.E. Thomposon, J. Appl. Phys. 79 (1996) 7991.
[10] P.W.M. Blom, M.J.M. de Jong, M.G. van Munster, Phys. Rev. B 55 (1997) 656.
[11] C.W. Tang, S.A. van Slyke, C.H. Chen, J. Appl. Phys. 65 (1989) 3610.
[12] T.A. Hopkins, K. Meerholz, S. Shaheen, M.L. Anderson, A. Schmidt, B. Kippelen, A.B. Padias, H.K. Hall Jr., N. Peyghambarian, N.R. Armstrong, Chem. Mater. 8 (1996) 344.
[13] S. Tolansky, Multiple Beam Interferometry of Surface and Films, Oxford University Press, London, 1988, p. 147.
[14] F. Abeles, M.L. Theye, Surf. Sci. 5 (1966) 325.
[15] M.M. El-Nahass, H.S. Soliman, N. El-Kadry, A.Y. Morsy, S. Yaghmour, J. Mater. Sci. Lett. 7 (1988) 325.
[16] S.Y. Kim, S.Y. Ryu, J.M. Choi, S.J. Kang, S.P. Park, S. Im, C.N. Whang, D.S. Choi, Thin Solid Films 398–399 (2001) 78.
[17] M.S. Xu, J.B. Xu, Synth. Met. 145 (2001) 177.
[18] M. Cölle, W. Brütting, Phys. Stat. Sol. (a) 201 (6) (2004) 1095.
[19] R. Shirley, The CRYSFIRE System for Automatic Powder Indexing: User's Manual, The Lattice Press, Guildford, Surrey, GU2 7NL, England, 2000.
[20] M. Brinkmann, G. Gadret, M. Muccini, C. Taliani, N. Masciocchi, A. Sironi, J. Am. Chem. Soc. 122 (2000) 514.
[21] B.H. Schechtman, W.E. Spicer, J. Mol. Spectrosc. 33 (1970) 28.
[22] G.A. Kumar, J. Thomas, N. George, B.A. Kumar, P. Radlhakrishnan, V.P.N. Nampoori, C.P.G. Vallabhan, Phys. Chem. Glasses 41 (2) (2000) 89.
[23] G.A. Kumar, G. Jose, V. Thomas, N.V. Unikrishnan, V.P.N. Nampoori, Spectrochim. Acta A 59 (2003) 1.
[24] M.M. El-Nahass, F.S. Bahabari, R. Al-Harbi, Egypt. J. Sol. 24 (1) (2001).
[25] M. Brinkmann, G. Gadret, M. Muccini, C. Taliani, N. Masciocchi, A. Sironi, J. Am. Chem. Soc. 122 (2000) 514.
[21] B.H. Schechtman, W.E. Spicer, J. Mol. Spectrosc. 33 (1970) 28.
[22] G.A. Kumar, J. Thomas, N. George, B.A. Kumar, P. Radlhakrishnan, V.P.N. Nampoori, C.P.G. Vallabhan, Phys. Chem. Glasses 41 (2) (2000) 89.
[23] G.A. Kumar, G. Jose, V. Thomas, N.V. Unikrishnan, V.P.N. Nampoori, Spectrochim. Acta A 59 (2003) 1.
[24] M.M. El-Nahass, F.S. Bahabari, R. Al-Harbi, Egypt. J. Sol. 24 (1) (2001).
[25] I.G. Hill, A. Kahn, Z.G. Soos, R.A. Pascal Jr., Chem. Phys. Lett. 327 (2000) 181.
[26] S.H. Wemple, M. DiDomenco, Phys. Rev. B 3 (1971) 1338.
[27] M.M. El-Nahass, Z. El-Gohary, H.S. Soliman, Optics & Laser Technol. 35 (2003) 523.